

Methane Detection using Optical Gas Imaging: Passive Infrared Technology

Abir Kebir, Hossein Emadi (Corresponding author), Dorcas Eyinla, and Humza Bin Navaid

Bob L. Herd Department of Petroleum Engineering, Texas Tech University

807 Boston Ave, Lubbock, TX 79409

E-mail: h.emadibaladehi@ttu.edu

Abstract

Methane (CH₄) is the dominant constituent of natural gas and plays a significant role in climate change as a powerful greenhouse gas. CH₄ lingers 30 times more than CO₂ in the atmosphere and has a greater potency in trapping heat. Human activities such as Oil and Gas production, underground mining, and landfill activities contribute to 25% to 33% of global warming worldwide. Traditional methods often lack real-time and accurate monitoring capabilities. To reduce the effect of methane emissions on global warming, several research works have demonstrated the efficiency of Passive Infrared Optical Gas Imaging in methane detection and quantification, which is widely used in Leak Detection and Repair programs (LDAR) as a non-destructive and non-invasive method. The combination of Machine Learning procedures such as Faster Region Convolutional Neural Network (Faster R-CNN) along with thermal infrared cameras was proven to be effective for methane detection and quantification. However, challenges remain in accurately determining emission rates. Recent studies have also revealed that methane emissions estimates provided by agencies like the Environmental Protection Agency (EPA) are often significantly underestimated. Recently, several detection projects demonstrated that the estimates the Environment Protection Agency (EPA) provided are underestimated. This paper explores the integration of machine learning models with optical gas imaging, examining methodologies, results, and limitations in methane detection across the petroleum industry, underground mining, and landfill sectors.

Future research directions include improving detection algorithms to enhance accuracy under varying environmental conditions, developing lower-cost sensor technologies for widespread deployment, and addressing regulatory challenges to ensure consistent and reliable methane reporting practices. This addition outlines promising future research areas and emphasizes key technical and regulatory challenges that must be addressed to advance methane monitoring capabilities.

Keywords: Greenhouse gas emissions, methane detection and quantification, Optical Gas Imaging, Infrared Technology, Faster R-CNN.

DOI: 10.7176/JETP/14-3-05

Publication date: October 30th 2024

1. Introduction

In recent years, observations of greenhouse gas emissions revealed a necessary urgency to monitor and reduce hazardous gas release in the air, such as methane, carbon dioxide, and nitrous oxide. Among these gases, methane overshadows all the other greenhouse gases because of its potency and occurrence across multiple fields, such as the petroleum industry, coal mining, and agriculture. Its concentration is increasing over time and attracting escalating concerns [1].

Methane leakage, therefore, is one of the most critical phenomena encountered in the industrial and environmental context. The increasing number of oil and gas wells in the world, particularly in the US, makes methane emissions hazardous, especially because methane is a greenhouse gas that lingers 10 years in the atmosphere before **Error! Reference source not found.** decomposition. Although released in smaller quantities than carbon dioxide, methane is roughly twenty-five times more effective at trapping heat [2]. Figure 1: 2022 U.S. Methane Emissions by source [3] shows that several sources cause the increasing quantities of methane leaks. Oil and natural gas systems, according to [3], are the source of 30% of the total emissions registered in 2022 in the U.S. taking place in all stages of the oil and natural gas industry from production operations to distribution. Gas production accounts for the highest percentage of leakage among the other segments, comprising 39% of emissions in the oil and gas industry [4,5]. Studies investigating most of the oil and gas wells in the New Mexico Permian revealed that 9% of the total production is leaked, while the EPA estimated that only 1.4% is leaked, proving that methane emissions are more hazardous than previously expected. Enteric fermentation and landfills [1] participate in 27% and 17% of emissions respectively; notably, Municipal Solid Waste (MSW) is considered

the third largest source of emissions caused by humans, comprising 14% of the total emissions in the U.S. in 2022. Reports indicating accurate emission rates of Greenhouse Gases (GHG) are obligatory for nations and individual landfills to monitor emissions [3,6]. Methane can be captured from landfills and used as a renewable energy source, 70% of which can be used for electricity and heat generation. Studies showed that around 200 Nm³/dry tons of CH₄ is generated by anaerobic biodegradation of municipal solid waste [7].

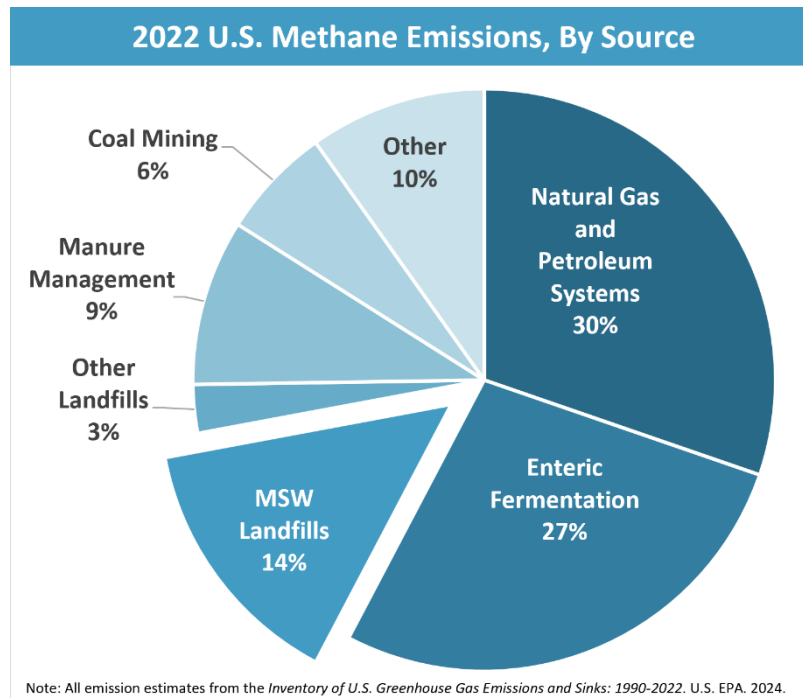


Figure 1: 2022 U.S. Methane Emissions by source [3]

U.S. Methane source [3]

Figure 1: 2022 U.S. Methane Emissions by source [3]

Several research works have tested the efficiency of multiple detection tools and methods. However, recent research focuses on pivots around thermal imaging found in infrared cameras. Passive infrared optical gas imaging is consistently used as a leak detection method as it provides high sensitivity to greenhouse gases, especially methane [8]. The convenience of optical gas imaging was proved in several studies [8-12,13] that showed the technology is qualitative and depends on the conditions in which thermal cameras are used. Some studies [2,14] affirmed that the emissions quantified by several research works are more critical than the quantities the Environmental Protection Agency estimated. The aspiration to mitigate methane emissions is based on developing robust sensors that can efficiently detect leaks. Other studies [31,32] focused on mathematical modeling and spectral imagers to measure the column density and methane concentration. However, these studies did not cover the use of conventional IR (Infrared) cameras as a quantification tool [115].

This paper addresses recent advances and technologies used in Optical Gas Imaging in the petroleum industry, mining, and landfill emissions, applications of infrared technology, and its limitations.

2. Optical Gas Imaging

Optical gas imaging (OGI) is an effective non-contact method that utilizes thermal cameras to create images and envision gases, including methane and different organic gases, mainly hydrocarbons [15,16]. Infrared cameras generate expeditious results when used to detect gas leaks and minimize fugitive gas emissions [17]. Their principle of operation is based on capturing the induced temperature in a certain frame and recognizing different wavelengths of infrared light that, when sufficiently intense, can emit heat (infrared radiation is directly proportional to the temperature of the object). The camera's internal measuring devices, called microbolometers, capture this thermal energy. Every pixel has one measuring device to measure and record the temperature and allocate every pixel to the appropriate color, showing the findings on the camera screen. Consequently, the captured data will be converted into an image that can be interpreted with the naked eye [18].

Optical Gas Imaging (OGI) is generally more cost-effective than traditional methane detection methods, particularly when considering its ability to provide rapid, non-contact inspections over large areas. Traditional

methods, such as flame ionization detectors (FIDs) and toxic vapor analyzers (TVAs), often involve point-based sampling, which requires physical proximity to leak sources and tends to be labor-intensive, time-consuming, and costly, especially in large-scale industrial settings. In contrast, OGI cameras can detect methane emissions visually from a distance, reducing the need for extensive labor and repeated site visits.

While the initial investment for OGI equipment, such as thermal infrared cameras, can be high, the long-term operational costs are lower. OGI allows operators to scan wide areas and detect leaks that would be missed by point-based sampling, thus avoiding the costs associated with undetected leaks, such as methane fines and lost products. Moreover, OGI enhances safety by allowing workers to remain at a safe distance from potentially hazardous gas emissions during inspections. Additionally, the ability of OGI to integrate with machine learning and automated detection systems can further reduce costs by minimizing the need for constant manual monitoring. As OGI technology continues to improve and becomes more widely adopted, these cost savings are expected to increase, making it an increasingly viable option for industries that rely on continuous methane monitoring.

Optical gas imaging, using infrared cameras, was combined with Convolutional Neural Networks (CNN) since Machine Learning models present extraordinary success in plume identification thanks to analysis enhancement and recognition of the gas flow patterns [19-21]. The purpose of this approach was to detect objects. Several research studies have been conducted on this topic; however, the first two generations of CNN (R-CNN and Fast R-CNN) were not applied to methane detection. Only the third one, Faster R-CNN, was applied along with infrared cameras to visualize methane. To develop an efficient model to detect leaks, Optical Gas Imaging registers a massive number of videos where leak recordings have been made to train the R-CNN Model and do the testing. The model's accuracy is conditional on the number of image proposals used for training, and the speed of treatment is sensitively harmed by large proposals [22,23]. Furthermore, it was proven that the detection accuracy is significantly affected by the imaging distance of the camera, which is considered the most important parameter. From an imaging distance of 10 m, 80% of emissions can be detected. Both elevated temperature and super emitters enhance detection accuracy; however, their influence is not as remarkable as the imaging distance [14].

One of the dominant methods in examining imagery is CNN, a type of deep neural network [24]. The use of CNN was significant in the 1990s. The primary model used was LeNet in 1989 by Lecun et al which focused on recognizing manually scripted digits [25]. Thereafter, it witnessed another renaissance in 2012, starting with AlexNet [26], then came [27] which trained a large and deep CNN to classify 1.2 million high-resolution images into 1000 classes—seemingly achieving a top 1 error rate of 37.5% as a top 5 error rate of 17%, which is considered a significant improvement. Despite this relative efficiency, they were still considered slightly expensive to be utilized on high-resolution images. However, using some GPUs (Graphics Processing Unit) coupled with a highly optimized implementation of 2D convolution was robust enough to ease the training of CNNs [27]. [28,29] developed and trained a CNN model to combine with OGI using TensorFlow software. The purpose was to assess the ability of GasNet (assembly of three CNN model variants) to effectively detect methane leaks and to differentiate between leak images and non-leak images. Building the CNN went through the ordinary method of construction as well as the image processing. They first used different leaking equipment to record around one million videos and collect labeled videos. The operation was conducted on various leak sizes ranging from 5.3 to 2051.6 g CH₄/h, as demonstrated in Table 1: Leak rates and the associated leak classes recorded from each imaging distance [29]. A variety of distances, from the source of the image to the source of the leak, ranges from 4.6 to 15.6 m. Then, the methane plume was extracted after testing different background subtraction methods. Finally, to locate the gas plume in the recorded video, the GasNet was tested.

Table 1: Leak rates and the associated leak classes recorded from each imaging distance [29].

Leak class label	Leak rate in scfh ($\pm 95\%$ CI)	Leak rate in g/h ($\pm 95\%$ CI)
Class 0	0.3 \pm 0.0	5.3 \pm 0.1
Class 1	16.8 \pm 0.1	277.7 \pm 1.1
Class 2	43.2 \pm 0.2	713.1 \pm 2.6
Class 3	58.1 \pm 0.2	958.8 \pm 3.1
Class 4	68.1 \pm 0.3	1124.3 \pm 4.3
Class 5	84.2 \pm 0.3	1389.8 \pm 4.8
Class 6	109.5 \pm 2.5	1806.1 \pm 41.4
Class 7	124.3 \pm 2.9	2051.6 \pm 48.0

The leak rates were recorded using a FLIR GF-320 Infrared camera generating many videos needed for CNN to train a deep learning network. The results of the study showed that the detection process became easier, and the

accuracy became higher, considering that the distance of the image and the strength of the plume signal in the images are inversely proportional. While dealing with large leaks (greater than 710 g CH₄/h) and installing the camera at a distance of 5 to 7 m, the accuracy is optimum and can exceed 97%. It was noticed that at the distance of 5 to 10 m, the accuracy is above 94%, while it decreases significantly at furthest distances of 13 to 16 m; however, if the leak is bigger (greater than 950g CH₄/h), the accuracy can reach 95% [29].

The US EPA recognized challenges related to quantifying emissions using OGI. [30] The Agency noted that one of the most important limitations of thermal IP cameras is their incapacity to measure the concentration of gas plumes. Several studies pointed out detailed limitations. [31] Hagen highlighted that while IR cameras can detect gas leaks, they are a recent invention and are still a subject of continuous research due to the challenges encountered. [32] Fox et al. demonstrated that the thermal cameras used to mitigate gas emissions do not give a quantitative assessment, they only give a qualitative assessment. [33] Implementing recent Artificial Intelligence (AI) assisted OGI systems developed by FLIR is limited to intelligent gas detection and segmentation.

Considering these limitations, the EPA suggests that additional devices should be used to quantify the emissions after an OGI system has detected and located the emission [34]. As a result, Almeida et al. [35] used an infrared gas analyzer to scrutinize the composition and concentration of gases; Ravikumar et al. [36] used the emission factor method [37] and the Hi-Flow sampler [38] to determine the emission rate. Al-hilal et al. [39] used flame ionization detectors (FID) or photoionization detectors (PID) for measuring gas concentration, and Gal et al. [40] used a combination of multiple devices (including an infrared gas analyzer, micro-chromatography, and the accumulation chamber technique) to quantify gas concentrations and flux. Moreover, Englander et al. [41,42] used laser absorption spectroscopy (LAS) [43] for column concentration measurements, and Lev-On et al. [44] characterized these OGI-assisted quantification methods into five types: average expected, leak/no leak, random sample screening, periodic screening, and high leaker sniffing.

The CNN algorithms were convenient for object classification since they were based on feature extraction and object classification [45], but they necessitated an additional step for further improvement. Object recognition was essential for the improvement of object detection using bounding boxes, which will eventually facilitate object detection [46]. This step will make the process more complex because instead of focusing only on object classification, it will assemble two different tasks: classification and recognition. This new technique is integral in the multistage detector group of the Region-Convolutional Neural Network, and it is divided into three different generations discussed in the upcoming sections [47]. CNN is not necessarily related to OGI and Infrared technology. However, the suggested models can be used and developed with OGI [48]. In particular, Faster R-CNN was the most widespread method combined with OGI for methane detection.

1.1. First Generation: R-CNN

R-CNN represents the commencement of all generations of R-CNN. It consists of three steps:

- 1- Propose region first by scanning the input image for possible objects using an algorithm called Selective Search, generating roughly ~2000 region proposals.
- 2- Run a convolutional neural network (CNN) on top of these region proposals to extract features.
- 3- Classify the features based on the features by taking the output of each CNN and feeding it into a) an SVM to classify the region and b) a linear regressor to tighten the bounding box of the object if such an object exists.

The main goal of this approach was to convert object detection into an indolent image classification task. That is why more expanded approaches were developed [47]. Girshik et al. suggested a new algorithm that could increase the Mean Average Precision (mAP) by more than 30% compared to the latest result, which was 53.3% registered on VOC2012. Their reasoning depended on coupling two main ideas to combine the region proposal with CNN. The first was to localize and segment objects; high-capacity CNNs can be applied to bottom-up region proposals. The second one was the application of supervised pre-training for an auxiliary, followed by domain-specific tuning, to generate an important improvement in performance when using rare labeled training data.

These studies' suggested system is illustrated in Figure 2: R-CNN Architecture [51]. The system attained a mean average precision of 53.7% on Pascal VOC 2010. When they compared this result to others previously registered (35.1% registered using a spatial pyramid and bag-of-visual-words approach, while 33.4% was registered when using the popular deformable part models), it was clear that R-CNN showed the best mAP. [49]. The R-CNN manifested drawbacks such as significant time waste, the need to provide a huge storage capacity, and outstanding computing performance. In addition to that, the multi-stage training pipeline contributing to this version is intricate. Consequently, the necessity to develop a more advanced generation of R-CNN was crucial to conquer the disadvantages of the previous generation. [49, 50].

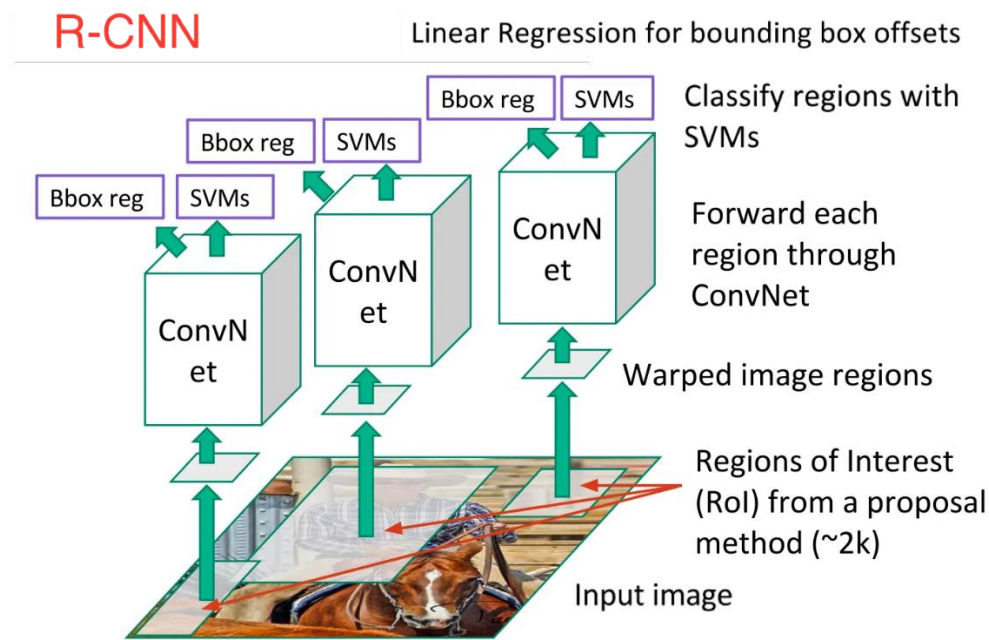


Figure 2: R-CNN Architecture [51]

1.2. Second Generation: Fast R-CNN

A year after the elaboration of R-CNN, Fast R-CNN, the second generation, was developed to address the issues found in the first generation. The particularity of this new generation compared to the first one is the integration of a new process called Region of Interest Projection (RoI projection). After feeding an image to the underlying CNN and launching the selective search, the coordinates of the bounding box are determined from the RoI Proposal and then projected while always respecting the subsampling ratio (the ratio of the feature map size to the original size of the image), into the feature map. The image used is a fixed-size image. The grid used for pooling is a 7x7 grid, and instead of employing the SVM (Support Vector Machine) classifier used in R-CNN, Fast R-CNN uses SoftMax [50].

This development shows an exponential improvement in the speed of training and testing. Unlike R-CNN, Fast R-CNN does not regularly feed 2000 region proposals to the convolutional neural network. The feeding operation is done once to create the feature map by feeding the input image to CNN. However, it shows a 66.9% accuracy on the PASCAL VOC 07 dataset, which is not considered good progress [50,51]. The results of the time consumption comparison between R-CNN and Fast R-CNN made by Aakarsh Yelisetty are shown in Table 2: Time consumption in R-CNN and Fast R-CNN [50] below:

Table 2: Time consumption in R-CNN and Fast R-CNN [50]

	R-CNN	Fast R-CNN
Training time	84 hours	9.5 hours
Speedup	1x	8.8x
Test time per image	47 seconds	0.32 seconds
Speedup	1x	146x
Test time per image with selective search	50 seconds	2 seconds
Speedup	1x	25x

Although Fast R-CNN significantly improved the training time and the image detection time, it still has a similar downside to R-CNN, consisting of the complexity of using selective search to extract 2000 region proposals in

which the objective was to reduce this amount. So, the faster R-CNN was implemented in object detection, mainly in methane detection. The major change was implementing a separate Neural Network to reduce the computational cost of object detection [52].

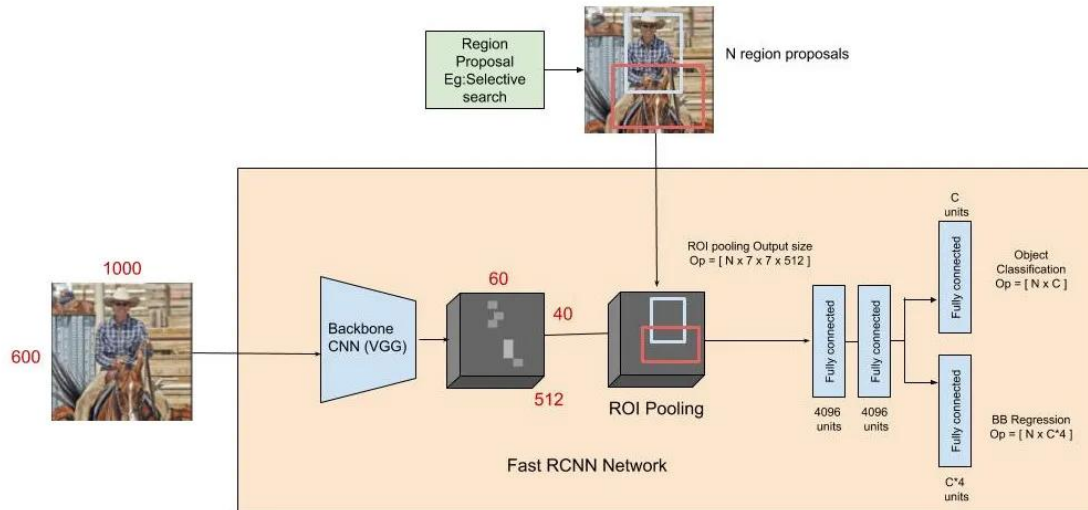


Figure 3: Fast R-CNN Architecture [52]

1.3. Third Generation: Faster R-CNN

To propose a region, Faster R-CNN had to use an independent neural network using CNN first to procure region proposals. Then, the predicted region proposal is reshaped using a RoI (Region of Interest) pooling layer. Subsequently, the image is classified within the proposed region, and the offset values for the bounding box are speculated by the RoI. A comparison between time consumption in the three generations is shown in Table 3: Time consumption in R-CNN, Fast R-CNN, and Faster R-CNN [52]: [51,52].

Table 3: Time consumption in R-CNN, Fast R-CNN, and Faster R-CNN [52]

	R-CNN	Fast R-CNN	Faster R-CNN
Test time per image with proposals	50 seconds	2 seconds	0.2 seconds
Speedup	1x	25x	250x
mAP (PASCAL VOC 07)	66.0	66.9	66.9

[22] stated that using OGI solely is a source of errors as it is ponderous. Manual analysis of the video frame can cause errors in interpreting the results. Therefore, they developed an automated model of hydrocarbon leak detection by integrating the Faster Region-Convolutional Neural Network (Faster R-CNN) that was first published in 2015 - a third generation of the Convolutional Neural Network Family- along with OGI. Faster R-CNN is the most extensively used approach among the R-CNN family. This approach is principally based on implementing the Regional Proposal Network (RPN) with Fast R-CNN. It considers that the RPN is the Regional Proposal Algorithm that will generate the Regional Proposal while the Fast R-CNN is the Detector Network. Implementing the RPN decreased the region proposal time from 2s to 10 ms per image. In addition, it collaborated in enhancing the feature representation as a consequence of sharing layers with the next detection stage [22, 53].

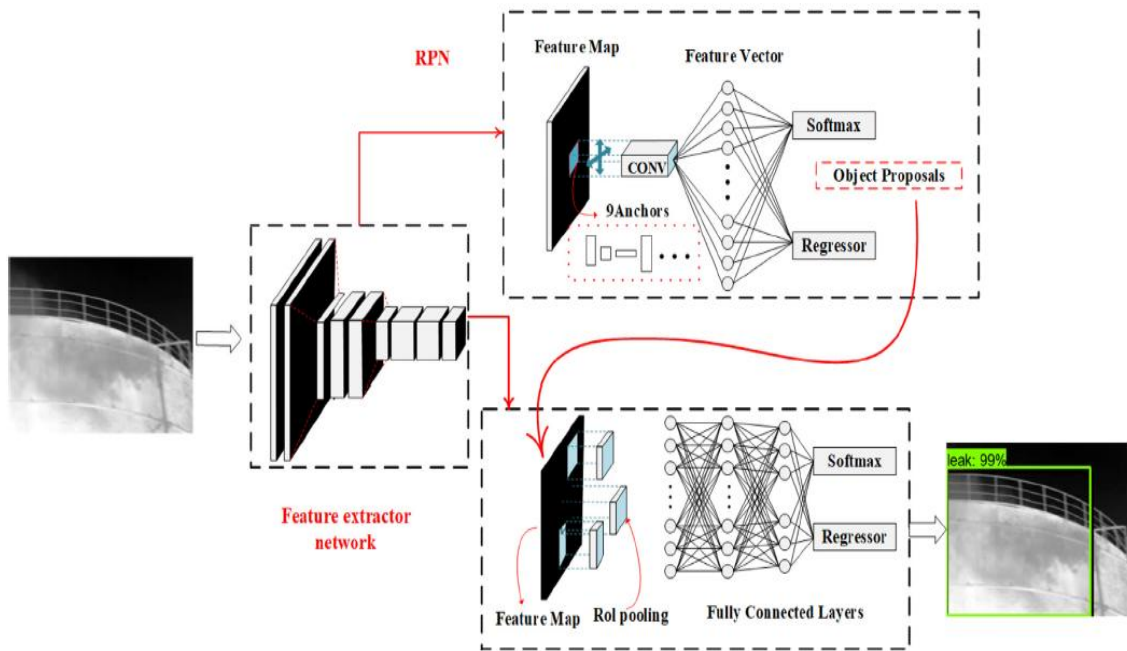


Figure 4: Faster R-CNN Architecture for Hydrocarbon leakage detection [22].

The RPN has a specific architecture containing a classifier and a regressor. The classifier. For the training purposes, the Loss Function is used:

$$L(\{p_i\}, \{t_i\}) = \frac{1}{N_{cls}} \sum L_{cls}(p_i, p_i) + \lambda \frac{1}{N_{reg}} \sum p_i L_{reg}(t_i, t_i) \quad (1)$$

$$L_{reg}(t_i, t_i) = \sum_{i \in \{x, y, w, h\}} smooth_{L1}(t_i - t_i), \quad (2)$$

$$smooth_{L1}(x) = \begin{cases} 0.5x^2 & \text{if } |x| < 1 \\ |x| - 0.5 & \text{otherwise,} \end{cases} \quad (3)$$

i is the Index of anchor,
 p_i is the predicted probability of being an object or not,
 t is a vector of 4 parameterized coordinates of the predicted bounding box,
 t_i is a vector of the ground-truth box,
 L_{cls} and L_{reg} represent the Log form of the classification Loss and the regression form, respectively,
 X, y, w and h represent the coordinates of the bounding box,
 N_{cls} and N_{reg} are the normalization terms,
 λ is 10 by default and is done to scale the classifier and regressor on the same level,
 p with regression term in the loss function ensures that if and only if an object is identified as yes, then only regression will count, otherwise, p will be zero, so the regression term will be equal to zero in the loss function [54].

[22] suggested a methodology that leads to an optimal Faster R-CNN joined with an Infrared camera to eventually detect leaks in real time of occurrence without the need for the intervention of humans (Figure 5: The proposed methodology to determine the optimal Faster R-CNN Model [22]). Their work showed that the exactitude of the Faster R-CNN is not directly influenced by the increasing depth of the feature extractor or by the reduction of the proposal number from 300 to 100 in this case. However, if the proposal number significantly decreases, the accuracy of the approach is remarkably damaged. On the other hand, the detection speed is directly related to and influenced by these parameters. The increasing depth of the feature extractor tends to slow down the detection speed while a lower proposal number improves the detection speed. According to the experiments, it has been found that the developed model based on Faster R-CNN and Resnet 101 coco with Resnet 101 feature extractor and 100 proposals is remarkably precise and secure than the Single Shot MultiBox Detector (SSD) models. One constraint in this approach is that the developed system could detect other systems with the same number of pixels as the leaks, which will probably cause erroneous results. In addition, if we want the accuracy of the manual annotation procedure to be improved, it is vital to implement an automated annotation technique. The main reason for these constraints is still unknown, but it may be due to the size of the dataset, the frame resolution, or the surrounding sounds. [23] Shi et al conducted another research study aiming to use Faster R-CNN with Infrared camera for real-time methane leak detection in offshore platforms. Although it is difficult to record many videos and execute real-time detection in offshore conditions, the experimental approach suggested that the thermal camera creates an ample number of virtual pictures using a Computational Fluid Dynamics (CFD) Simulation tool as a cost-effective method. The Faster R-CNN model was then trained and tested to minimize the Loss Function.

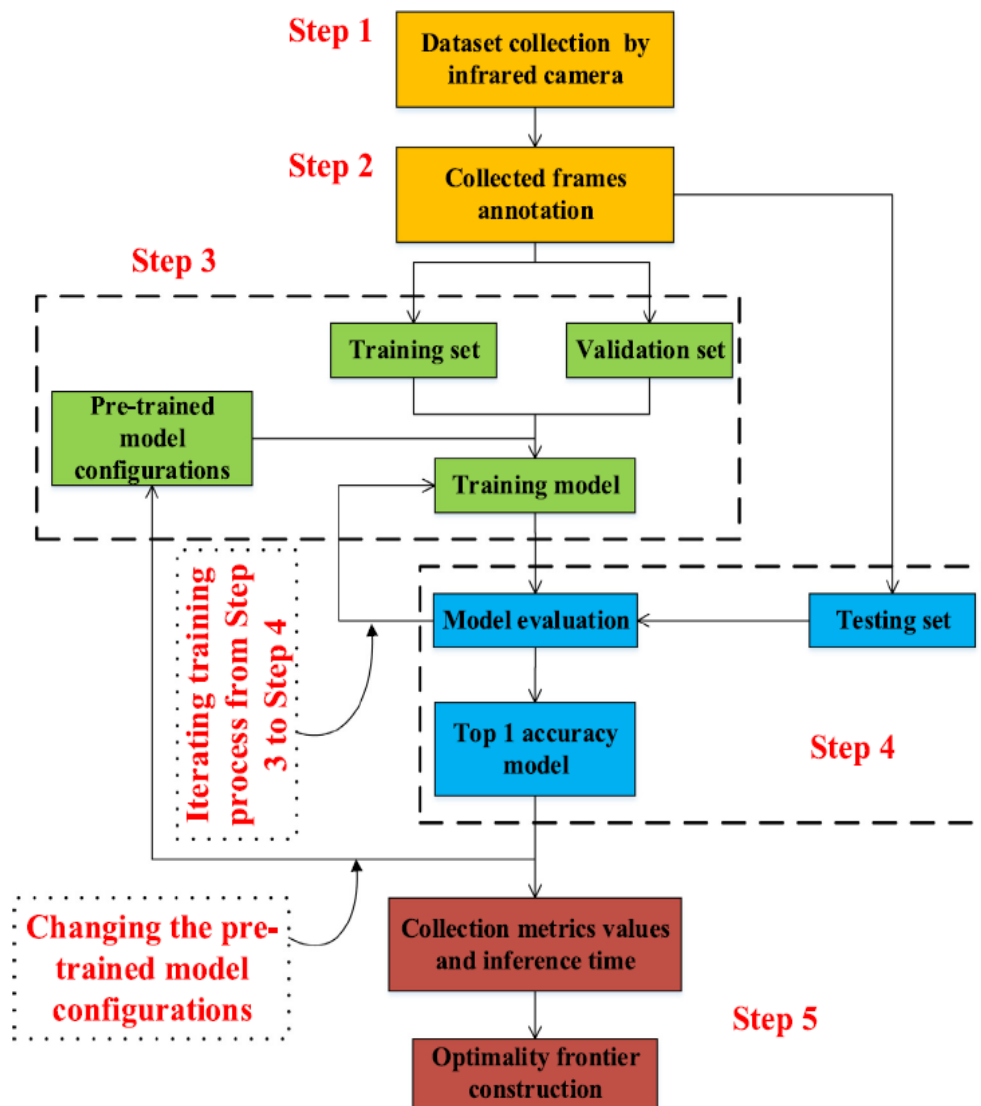


Figure 5: The proposed methodology to determine the optimal Faster R-CNN Model [22]

Recent advancements in Convolutional Neural Networks (CNNs) have significantly enhanced methane detection applications, particularly when combined with Optical Gas Imaging (OGI) technology. CNNs excel at image recognition tasks, making them highly effective for identifying methane leaks in infrared imagery. With improved architectures, such as Faster R-CNN, CNNs can detect leaks with greater accuracy and speed, even in challenging conditions with complex backgrounds or low contrast.

The improvements in CNN algorithms benefit methane detection by enhancing the precision of leak localization, enabling real-time detection and quantification of emissions. Advanced CNNs can be trained on large datasets to recognize the unique thermal signatures of methane leaks, allowing the models to distinguish methane from other gases or environmental features, reducing false positives. Additionally, optimized CNNs require less computational power, which facilitates on-site processing and integration into portable devices, making methane monitoring more efficient and accessible across various industries.

3. Applications of infrared technology in methane detection

While thermal imaging is used in various fields such as electrical maintenance, plumbing, mechanical and building construction, transport navigation, and health care and medicine, infrared technology is showing great potential in

methane detection and quantification, especially for accurate real-time results. Multiple academic research works have been conducted to test the efficiency and applicability of infrared cameras in detecting and quantifying CH₄ in different sites and locations [55].

Traditional sensors, such as laser detectors, could only indicate that the pre-defined gas threshold had been exceeded but could not delineate the source of the leak [23]. Infrared sensors, contrariwise, can precisely indicate the location of the leak. The US Environmental Protection Agency (EPA) indicated, through a comparative study of different optical technologies, that Infrared Optical Gas Imaging is the current efficient technology that could potentially replace current Leak Detection and Repair (LDAR) techniques [15,30]. The atomic and molecular weight of the gas determines the absorption rate of certain light waves. The wavelengths range from 2200 nm to 2400 nm as shown in Figure 6 can be absorbed by CH₄ in a distinctive pattern called a spectral fingerprint. For larger methane plumes, the absorption is higher which results in a higher intensity of the signal [56, 57].

Infrared technology is used as a non-destructive precise gas sensing method based on thermal wave imaging. It absorbs the light emitted from a source and uses an optical transducer for the measurement of the signal [57]. This technology has recently witnessed a large spread in both academia and industry. [58] Joyce et al. used the PRecursore IperSpettrale della Missione Applicativa (PRISMA) satellite to localize the source of methane plumes and quantify methane emissions from different human activities. This method proved successful in locating and quantifying methane plumes in quasi-real time from 30m resolution satellite data and ultimately alleviate emissions in the atmosphere.

Methane spectral fingerprint

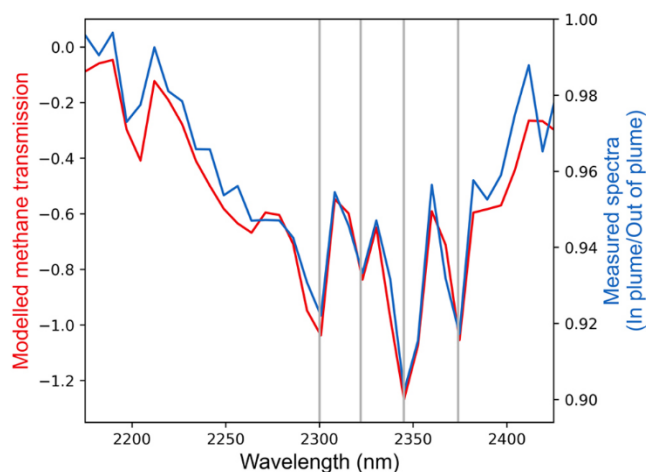


Figure 6: Methane spectral fingerprint [57].

[59] NASA, in a new space mission, initiated Earth Surface Mineral Dust Source Investigation (EMIT) to send on a space mission. These detectors were initially used to investigate the effect of dust on weather patterns; however, they can also be employed to spot methane emissions. In addition to precisely spotting the location of the leaks, this pristine technology will also mitigate against methane exhaust. The collection of data is executed in desert areas on five different continents: Africa, Asia, Australia, and North and South America. However, what they called “Super Emitters” were found only in two continents: Asia and America. The biggest leaks were mainly a result of the waste from fossil fuel activities (facilities, equipment, and oil and gas infrastructures) and agriculture activities. The effectiveness of infrared detection varies depending on climate conditions. Temperature has a great effect on efficiency. According to a study conducted by Wang et al. [60], the detection uncertainty decreases when the ambient temperature is low and vice versa.

3.1. Oil and Gas Industry

Optical Gas Imaging using infrared cameras can also be utilized in the petroleum industry, specifically in offshore platforms, even though it represents a challenge [61]. A bi-annual monitoring frequency in onshore and offshore well sites is mandatory using Optical Gas Imaging as the Best System of Emission Reduction (BSER). This technology works by generating a fading wave from infrared light. It is used to detect the presence and measure the concentration of dissolved CH₄ in seawater. [23] Due to the scarcity of CH₄ fugitive discharges, it was challenging to record many videos using OGI solitary in deep water drilling offshore platforms. Hence, it was required to combine infrared cameras with faster R-CNN to generate virtual images for instantaneous detection.

[62] Ravikumar et al tested the performance of a commercial infrared camera while considering environmental effects and imaging conditions. They conducted the experiments in the Methane Emissions Technology Evaluation Center (METEC) at Colorado State University. The center where the study was applied perfectly mimics a natural gas exploration area with the following components: wellheads, separators, and tank batteries. The gas was flowing from a cylinder at a pressure of 2500 psi, and it leaked through several leaks existing in every component.

[63,64] Another study was performed on 128 plugged and 206 unplugged abandoned wells in the state of Colorado in the United States, which showed that plugged wells emit 0 g ch₄ well⁻¹ h⁻¹; however, unplugged wells emit an average of 586 g ch₄ well⁻¹ h⁻¹ whereas the first super-emitting abandoned well was found at a rate of 76 kg ch₄ well⁻¹ h⁻¹. The average methane quantity found in the atmosphere in this study is 75 times larger than the current US average of gas emissions. At the United States level, collected data showed methane rates emissions from abandoned wells in five different American states. The results are shown in Table 4.

Table 4: Methane rates in abandoned wells in 5 states in the United States [63]

US State	Number of wells	CH ₄ rate (g ch ₄ well ⁻¹ h ⁻¹)
Pennsylvania	40	12
Oklahoma	20	4
California	97	0.3
West Virginia	112	0.1
Ohio	6	0

Satellites are considered efficient tools for recognizing large greenhouse sources. [65] A FLIR Gas Finder 320 infrared camera was used in the borders between Arizona and California in a single-blind fixed location study to evaluate methane sensing systems designed for point-source real-time detection and quantification and to follow the dispersion of the gas plume. The team used a flowing liquified natural gas from a van directly to a heater trailer and then to a metering and releasing trailer. This installation was an imitation of an oil and gas flaring system of a production field. The results of this study showed that the satellites could detect most emissions and did not report any false positives.

[66] To identify any potential sources of flowing gas in the atmosphere, Allen et al used infrared cameras to look over four different natural gas production sites in the United States and to identify the source of the leak according to the work practice 40C FR 60.18. The method used could detect a methane threshold of 30g/hr. Those sites include Appalachian, Gulf Coast, Midcontinent, and Rocky Mtn. The measurement was made at 189 gas wells, and the study could only measure methane leaks during the completion phase. Further studies should be done during the production phase to determine the total rate of methane emissions during oil and gas production using the same method since the measurement uncertainties are not significant. [67] Furthermore, Brown et al worked on an estimation of methane emissions in midstream. In six months, they evaluated the gas outflows using several technologies, including OGI and LDAR. The main goal was to correlate the flow rate of emissions with operation and maintenance events. It was found that, in operating conditions, top-down techniques are less likely to be as efficient as bottom-up techniques for midstream facilities. Additional testing should be completed to further compare top-down and bottom-up techniques. [9,68] In oil and gas wells, a comparison between ground and aerial surveys demonstrated that the detected methane rates were significantly higher when the first method (Ground survey) was implemented. The responsiveness of the ground survey tool is superior; however, the effectiveness will be affected by ambient temperature. Additionally, it was demonstrated that the leakage frequency from storage tanks is greater, [10,11] which signifies that the control and mitigation of fugitive emissions from this source will considerably reduce methane and volatile organic compounds (VOC) emissions. [10] An evaluation of VOC and Hazardous Air Pollutants (HAPs) emissions revealed that both on-site and remote measurements gave the same results. However, results obtained when a High-Volume Sampler (HVS) was used were underestimated.

Transmission and storage systems of natural gas in the US also play a crucial role in methane emissions. A quarterly monitoring frequency is mandatory using Optical Gas Imaging as the best BSER (Best System Of Emissions Reduction). [69-70] It was shown that the largest emission sources were fugitive emissions from certain compressor-related equipment and “super-emitter” facilities. The total methane emissions estimate from the Transmission and Storage sector were at 1,503 [1,220 to 1,950] Gg/yr compared to the 2012 EPA’s Greenhouse Gas Inventory (GHGI) estimate of 2,071 [1,680 to 2,690] Gg/yr. The confidence level of their estimate was 95%. During gathering and processing operations, the CH₄ loss rate was estimated to be 2421 (+245/-237) Gg, representing 0.47% (±0.05%) loss for all the U.S. The source of these emissions was the primarily normal operation of gathering facilities followed by the operation of processing plants. The estimates were 1.7 times lower than the 2012 EPA Greenhouse Gas Inventory (GHGI) estimate for processing plants; however, they were 3 times higher

than the EPA Greenhouse Gas Reporting Program. Since not all CH₄ emissions are reported, a significant difference is registered in gathering operations emissions. These emissions represent 30% of the total estimate. [71] It is suggested to combine Tunable Laser Spectroscopy (TLS) with mid-infrared imaging as a sensitive method to visualize the gas plume.

Gas pipelines demonstrate high leakage rates of methane. [72] The Environmental Defense Fund (EDF) announced that methane leaks originating from natural gas pipelines are estimated to be 2.6 million tons yearly representing the equivalent emissions of 50 million cars operating for a year. EDF also indicated that the U.S. Environmental Protection Agency’s Greenhouse Gas Inventory estimates of methane leaks from pipelines are significantly underestimated. [73-80] Thermal imaging and multi-wavelength imaging, in this case, represent a major advantage as they can be used from the ground, vehicle, aircraft, and satellite platforms. Table 5 represents a comparison between annual methane leaks reported by EDF and EPA from U.S. gas pipelines.

Table 5: Annual methane emissions from U.S. pipeline leaks [72]

ANNUAL METHANE EMISSIONS FROM U.S. PIPELINE LEAKS IN METRIC TONS		
	EDF	EPA 2022
Gathering pipelines	482,000 – 1,890,000	127,000
Transmission pipelines	6,400	3,300
Distribution pipelines	761,000	203,000
Total	1,250,000 – 2,660,000	333,000

The estimates provided by EDF and EPA demonstrate the quantification gap related to methane emissions, referring to differences in the methods, technologies, and data collection used by both entities. The primary reason for the rate difference could be that EPA uses periodic inventories provided by companies. However, EDF uses satellite imagery, ground-based imagery, and air-based imagery for real-time emission data, providing a comprehensive representation of real methane rates.

3.2. Underground mining

[81] Lorenzo-Bayona et al made an experimental comparison of some methane sensors used in underground coal mining. The study’s objective was to test the efficiency of the key methane sensing technologies, such as laser and LDAR, used to bolster safety measures in this kind of environment. The factors taken into consideration that could affect the operation process of the sensors are the temperature, pressure, time taken to respond, and dust influence. The EN 60079- 29-1 standard, one of the standards of Directive 2014/34/EU of the European Parliament and of the Council of 26 February 2014, was applied on 10 mobile devices and six non-mobile devices to have a total of 16 methane sensors. If the infrared sensors are not supplied with a temperature sensor, a calibration should be executed to match the operation temperatures [82].

It was found from [81] that optical sensors always have the highest response time compared to interferometric sensors were found inaccurate because weather conditions highly impact them and also catalytic sensors were found to be untrustworthy when the sensing operation is applied on low methane concentration in a long period or when it is applied on high methane concentration in a short time. According to this study, infrared sensors are not influenced by oxygen concentration changes. However, they are significantly influenced by the pressure change as well as the presence of humidity in the air which causes the dilution of gas and affects the photonic absorption of the infrared light by the gas. Ethane is another factor affecting infrared functioning since its presence decreases its efficiency by 10%.

3.3 Landfills gas emissions

The constant growth of the number of landfills across the world is due to industrial, human, and agricultural activities. Solid Waste disposal produces around 20% of the total methane in the air [1,83]. In landfill gas emissions (LFG), the gas is composed of 40-60% of methane, 40-50% of CO₂, and the rest is composed of some other gases present in a small amount. Most landfill gas detection was executed using ground-based screening tools; however, remote sensing screening tools have been utilized more in recent years. [84] Since the anaerobic digestion process is sensitive to ambient conditions and surrounding changes, traditional methods used by biogas plant operators were not practical due to the complexity of monitoring the process. Henceforth, machine learning algorithms were developed to be implemented in anaerobic digestion to monitor and optimize biogas production. [85,86] The passive infrared camera is effective not only in detecting methane emissions from landfills but also in detecting temperature variations caused by aerobic respiration during the day and the night. If the surface temperature from the airborne Long-Thermal Infrared (LWIR) can be precisely corroborated and mapped with surface temperature measurements, high surface temperature, and high methane concentration areas can be identified. [87,88] Methane

indices included Particular Narrow Spectral SWIR ranges such as 1630 – 1699 nm and 2100 – 2300 nm to localize high methane concentration areas. [89] Infrared absorption spectra experiments using Fourier Transform Infrared Spectroscopy in the wavelength range of 1.0 to 1.7 μm enable the real-time determination of CH_4 concentrations. [90,91] In Melbourne, Australia, Lewis et al focused on the adaptability and constraints of infrared thermography to measure gas leakage emitted from landfills by investigating the effect of weather, ground conditions, and sensor-leak distance. The work targeted the potential leak spots and used the Thermal Infrared Spectroscopy (TIR) by taking pictures with a camera of 320 x 240 pixels resolution and a field of view of $24^\circ \times 18^\circ$. The camera used could not successfully detect all the leaks. The temperatures read by the camera and the thermometer were different in the presence of the same methane concentration. Therefore, other factors such as light, wind, and barometric pressure significantly affected the detection accuracy. Under windy weather, the temperature tends to decrease when using TIR, so the concentration of methane detected was insignificant (less than 0.03%). Apropos of the ambient temperature, in cooler temperatures, the camera can demonstrate higher accuracy in detecting methane leaks as an abnormality. While in higher temperatures, the leak could not be recognized. The surface material can also play a role in confusion. In some cases, plastic bags can be misinterpreted as landfill gas leaks. [92] Fjelsted et al used the same method in Denmark in two landfill areas of 100 m^2 fragmented into 100 measurements. The same type of camera was used but with a different resolution of 382 x 288 pixels. The outcomes revealed that the method had the same temperature differences as the previously mentioned method. Moreover, the emission rate must be greater than 150 $\text{g CH}_4 \text{ m}^{-2} \text{ d}^{-1}$ and the area must be greater than 1 m^2 . Another successful experiment conducted by [93] Tanda et al. demonstrated that the use of unmanned flight vehicles (UAVs) in landfill surfaces is successful in determining thermal anomalies recorded on a large piece of surface. The aerial infrared photographs explicitly showed the thermal anomalies generated from biogas digestion. Thus, the method was efficient in revealing accurate biogas production from urban waste disposals.

[94] It was proved that the prediction of CH_4 is contingent upon temperature anomalies of the ground as well as solar radiation in in-situ conditions. Low rates of untreated methane constitute a powerful source of greenhouse gas. [95] Tian et al. highlighted the importance of low methane content landfill gas mitigation. A photocatalyst, $\text{Y}_2\text{O}_3:\text{Er}^{3+}-\text{TiO}_2-0.05\%$ graphene (GR) was combined with the sol-gel method. When exposed to visible near-infrared sunlight, the experiment showed a good response, promising a practical alternative to the classic photocatalytic degradation technology that depends on ultraviolet (UV) light. [96] Njoku et al. investigated the influence of meteorological conditions on subsurface emissions using a government-accredited GA 2000 landfill gas analyzer. The subsurface CH_4 concentrations are inversely proportional to the distance from the landfill activities and CH_4 migrates to shallower depths towards the soil surface through pores. It was found in this study that carbon dioxide was present in larger concentrations compared to methane. [97] Therefore, for isolation purposes, a bottom base sealing is always mandatory to prevent the migration of any gas and water from the landfill base to the atmosphere and to deeper depths. Additionally, an HDPE (High-Density Polyethylene) piping system is used to recuperate and direct the generated gas to treatment units to be used in energy regeneration.

Previous studies show that passive infrared imaging models can accurately produce infrared images in the petroleum industry and landfills especially when the leak rate is sufficiently high. The technology is a valuable tool for leak identification. However, further studies should be conducted to estimate the gas leak rate, particularly when the rate is low.

4. Contrast between thermal passive infrared detection and laser detection

Thermal Passive infrared and laser technologies can be used with drones to detect and measure hazardous methane leaks. However, their fundamental operating mechanism is entirely different. The main difference resides in the type of detection. While infrared cameras detect a leak in a wide area, the laser detector detects only a spot in a narrow field of view of one point.

Both can be equally efficient in detecting dangerous gas leaks mounted on drones, but they are based on different principles and serve various purposes. Methane absorbs specific wavelengths. This absorption reduces the infrared radiation that hits the detector, thus indicating the existence of gas. The mid-IR region is often referred to as the 'molecular fingerprint' region of the electromagnetic spectrum because molecules can be uniquely identified from their spectral signatures. This opens applications in a range of fields from environmental monitoring to health and medical diagnostics, industry, security, and defense. The mid-IR range also spans the spectral peak of thermal emissions from most biological and mechanical objects with temperatures between 200 K and 1400 K. This spectral range is, therefore, critical for security and defense applications aimed at thermal targeting and night vision, as well as for energy auditing and conservation [98-102].

Optical gas sensors that work based on LAS (Laser Absorption Spectroscopy) are typically combined with multi-pass gas cells, optical resonators—cavities—and photoacoustic spectroscopy [103-105]. The most advanced and universal optical technique for gas measurement is tunable diode laser spectroscopy (TDLS). TDLS can be used

for in situ and remote measurements. This technique is now capable of detecting trace gas concentrations with sensitivities at the parts-per-trillion (ppt) level [106-110]. In the Tunable Diode Laser Technique (TDLA), the wavelength of a single line emission of a laser diode is scanned precisely over a single gas absorption line, and the peak absorption at the line center is compared to the baseline on either side of the line [111]. In laser sensor-based technology, the gas beam may be pointed at different targets, such as gas pipelines, gas piping systems, or even the ground. A diffused ray will reflect back from the objective after directing a primary laser beam to the same objective. Eventually, the device will collect the imitated beam, quantify the absorptivity of the light ray after receiving it, and give a final result of the methane column density (ppm-m). According to Works Well, there are higher chances of locating a hazardous gas leak using an infrared camera than using a laser detector. The other advantage of using a thermal camera is reducing the time needed to locate the same gas leak. Further differences are shown in Table 6.

Table 6: Differences between Infrared and Laser Technologies [64,112-114]

	Passive Infrared	Laser
Principle technology	<ul style="list-style-type: none"> Infrared source light and filter technology 	<ul style="list-style-type: none"> Near-infrared laser technology
Spectrum	<ul style="list-style-type: none"> Only weak resolution is achieved 	<ul style="list-style-type: none"> High resolution is achieved therefore there is no resolution problem
Long term stability	<ul style="list-style-type: none"> Infrared light life is similar to the life of light bulbs. It becomes less potent progressively due to aging. 	<ul style="list-style-type: none"> Longer operating life thanks to the adoption of the latest and the steadiest semiconductor photoelectric components.
Single channel stability	<ul style="list-style-type: none"> IR sensors need a second measurement channel as a reference Regular calibration is required to avoid any issues and further complications which may lead to erroneous results 	<ul style="list-style-type: none"> No necessity for regular calibration or a reference channel. The laser detector has long-term stability with only a single channel
Detectable gases	<ul style="list-style-type: none"> Variety of gases (more than 100 gases) 	<ul style="list-style-type: none"> Exclusively one gas
Type of measurement	<ul style="list-style-type: none"> Image stream (the area where the leak is found) Infrared sensor measures the dissemination of gas and the point of release for a leak Thorough scanning of a complete area 	<ul style="list-style-type: none"> Spot measurement (Just one spot, not an area) Only the presence of gas Liner inspection
Power consumption	<ul style="list-style-type: none"> High power consumption 	<ul style="list-style-type: none"> The laser diode in the laser detector emits 100% of its light and consumes less energy.
Response time	<ul style="list-style-type: none"> A relatively high response time that takes more than 30 seconds due to the utilization of only a small amount of effective Infrared radiation. 	<ul style="list-style-type: none"> Response time varies from 6 seconds to 8 seconds for a laser-type methane sensor.
Humidity	<ul style="list-style-type: none"> Water molecules demonstrate a noteworthy absorption capacity in the Infrared range, resulting in an impotent infrared response. Infrared sensors are affected by the ambient temperature as well. 	<ul style="list-style-type: none"> Laser sensors do not absorb vapor; therefore, they do not exhibit any response for water molecules and demonstrate efficient vibration resistance. Laser sensors are not affected by the ambient temperature as well.

5. Limitations and Conclusions

At the moment, one of the greatest threats to environmental sustainability is methane, which is caused by uncontrolled emissions in different industries. Earth observation fully supports the monitoring of the abundant greenhouse gas emissions. Traditional methane detection methods often fall short in providing accurate, real-time data, highlighting the need for advanced technologies. Passive Infrared Optical Gas Imaging, coupled with machine learning algorithms like Faster R-CNN, has shown promise as an effective, non-destructive tool for methane leak detection and quantification. This paper reviewed the methodologies and challenges associated with these technologies across various sectors, indicating that current estimates of methane emissions may be significantly underestimated. From the previously mentioned studies, several limitations were revealed:

- (1) Non-pure gases, especially the ones with higher molecular weight result in a lower detection threshold. Oil and gas production and processing produce a mixture of gases in the quasi-totality of the cases. Moreover, wet gas is responsible for reducing the detection threshold compared to the cases where only dry gas is leaked.
- (2) Meteorological conditions such as low temperature and high wind velocity constrain the cameras to localize and quantify the leak. Therefore, detection is more efficient in warmer weather and low wind velocities.
- (3) Water molecules demonstrate a noteworthy absorption capacity in the Infrared range, resulting in an impotent infrared response. Therefore, low levels of humidity are favorable for accurate estimates and precise determination of the gas plume.
- (4) Localizing and quantifying gas leaks at low rates and distances are still challenging. The detection range is limited to short distances (lower than 5 m) from the leak source to the camera's location which could represent a challenge in big industrial plants. Machine learning tools were efficient in localizing gas plumes; however, the development of the Faster R-CNN method is still needed for intermittent emissions and low emission rates.

Improving passive infrared technology to be more reliable and applicable for methane detection and quantification, to make better environmental management and mitigation strategies possible, requires overcoming these limitations through advanced research and development. The ultimate goal is to develop technologies and systems that are accurate, robust, convenient, and cost-effective to make them suitable for engineering practice. The developments would be designed to enhance the capabilities of the present gas analysis and spectroscopic techniques. This emphasizes the need for interdisciplinary research that integrates developments in artificial intelligence, machine learning, and data science, extend 2D IR images to 3D spectral ones combined with spectroscopy, and leverages the global structure information by AI to make concentration and emission rate data from IR images. The refinement of these technologies is essential to contribute to global efforts in addressing climate change.

Future research directions in this field should focus on enhancing detection algorithms to improve accuracy under diverse environmental conditions, developing cost-effective sensor technology to facilitate broader deployment, and addressing regulatory inconsistencies that impact methane reporting practices. Tackling these areas will be crucial for refining methane monitoring systems, reducing emissions, and mitigating the environmental impact of this potent greenhouse gas.

References

[1] Izzet Karakurt, Gokhan Aydin, Kerim Aydiner, Sources and mitigation of methane emissions by sectors: A critical review, *Renewable Energy*, Volume 39, Issue 1, 2012, Pages 40-48, ISSN 0960-1481, <https://doi.org/10.1016/j.renene.2011.09.006>.

[2] <https://news.stanford.edu/press-releases/2022/03/24/methane-leaks-mues-fix-available/>

[3] Basic Information about Landfill Gas, United States Environmental Protection Agency, [Online], Available: [https://www.epa.gov/lmop/basic-information-about-landfill-gas#:~:text=Landfill%20gas%20\(LFG\)%20is%20a,of%20non%2Dmethane%20organic%20compounds](https://www.epa.gov/lmop/basic-information-about-landfill-gas#:~:text=Landfill%20gas%20(LFG)%20is%20a,of%20non%2Dmethane%20organic%20compounds)

- [4] Primary Sources of Methane Emissions, [Online], Available: <https://www.epa.gov/natural-gas-star-program/primary-sources-methane-emissions>
- [5] Estimates of Methane Emissions by Segment in the United States, [Online], Available: <https://www.epa.gov/natural-gas-star-program/estimates-methane-emissions-segment-united-states>
- [6] Oonk, H. (2010). Literature review: methane from landfills. Final report for Sustainable landfill foundation.
- [7] Nickolas J. Themelis, Priscilla A. Ulloa, Methane generation in landfills, *Renewable Energy*, Volume 32, Issue 7, 2007, Pages 1243-1257, ISSN 0960-1481, <https://doi.org/10.1016/j.renene.2006.04.020>.
- [8] Daniel Zimmerle, Timothy Vaughn, Clay Bell, Kristine Bennett, Parik Deshmukh, and Eben Thoma, Detection Limits of Optical Gas Imaging for Natural Gas Leak Detection in Realistic Controlled Conditions, *Environmental Science & Technology* 2020 54 (18), 11506-11514, DOI: 10.1021/acs.est.0c01285
- [9] Lyman, SN, et al. 2019. Aerial and ground-based optical gas imaging survey of Uinta Basin oil and gas wells. *Elem Sci Anth*, 7: 43. DOI: <https://doi.org/10.1525/elementa.381>
- [10] Halley L. Brantley, Eben D. Thoma & Adam P. Eisele (2015) Assessment of volatile organic compound and hazardous air pollutant emissions from oil and natural gas well pads using mobile remote and on-site direct measurements, *Journal of the Air & Waste Management Association*, 65:9, 1072-1082, DOI: 10.1080/10962247.2015.1056888
- [11] Lyon DR, Alvarez RA, Zavala-Araiza D, Brandt AR, Jackson RB, Hamburg SP. Aerial Surveys of Elevated Hydrocarbon Emissions from Oil and Gas Production Sites. *Environ Sci Technol*. 2016 May 3;50(9):4877-86. doi: 10.1021/acs.est.6b00705. Epub 2016 Apr 15. PMID: 27045743.
- [12] Subramanian R, Williams LL, Vaughn TL, Zimmerle D, Roscioli JR, Herndon SC, Yacovitch TI, Floerchinger C, Tkacik DS, Mitchell AL, Sullivan MR, Dallmann TR, Robinson AL. Methane emissions from natural gas compressor stations in the transmission and storage sector: measurements and comparisons with the EPA greenhouse gas reporting program protocol. *Environ Sci Technol*. 2015 Mar 3;49(5):3252-61. doi: 10.1021/es5060258. Epub 2015 Feb 10. PMID: 25668051.
- [13] why a natural gas initiative in Natural Gas Initiative GI by Stanford University (2015), <https://ngi.stanford.edu/>
- [14] Arvind P. Ravikumar, Jingfan Wang, and Adam R. Brandt, Are Optical Gas Imaging Technologies Effective For Methane Leak Detection?, *Environ. Sci. Technol*. 2017, 51, 1, 718–724, November 29, 2016, <https://doi.org/10.1021/acs.est.6b03906>
- [15] Kang, R.; Liatsis, P.; Kyritsis, D.C. Emission Quantification via Passive Infrared Optical Gas Imaging: A Review. *Energies* 2022, 15, 3304. <https://doi.org/10.3390/en15093304>
- [16] Safitri, A. (2011). *Infrared optical imaging techniques for gas visualization and measurement* (Order No. 3471335). Available from ProQuest Dissertations & Theses Global. (885772763).
- [17] Optical Gas Imaging with Infrared Technology, [Online], Available: <https://infraredcameras.com/industries-served/optical-gas-imaging/>
- [18] How does thermal imaging work, [Online], Available: <https://www.pyrosales.com.au/blog/news/how-does-thermal-imaging-work/#:~:text=Thermal%20cameras%20detect%20temperature%20by,ways%20that%20heat%20is%20transferred>

- [19] Yoojin Jung, Byunghyun Han, M. Erfan Mostafid, Pei Chiu, Ramin Yazdani, Paul T. Imhoff, Photoacoustic infrared spectroscopy for conducting gas tracer tests and measuring water saturations in landfills, *Waste Management*, Volume 32, Issue 2, 2012, Pages 297-304, ISSN 0956-053X, <https://doi.org/10.1016/j.wasman.2011.09.016>.
- [20] Navaid, Humza Bin and Emadi, Hossein and Eyinla, Dorcas S. and Kebir, Abir, Machine Learning Insights for Safer Subsurface Fluid Injection: Predictive Analysis of Injection Induced Seismic Precursor Environments. Available at SSRN: <https://ssrn.com/abstract=4608110> or <http://dx.doi.org/10.2139/ssrn.4608110>
- [21] Dorcas Eyinla, Steven K. Henderson, Hossein Emadi, Sugan Raj Thiyagarajan, Aman Arora, Optimization of hydraulic fracture monitoring approach: A perspective on integrated fiber optics and sonic tools, *Geoenery Science and Engineering*, Volume 231, Part B, 2023, 212441, ISSN 2949-8910, <https://doi.org/10.1016/j.geoen.2023.212441>.
- [22] Jihao Shi, Yuanjiang Chang, Changhang Xu, Faisal Khan, Guoming Chen, Chuangkun Li, Real-time leak detection using an infrared camera and Faster R-CNN technique, *Computers & Chemical Engineering*, Volume 135, 2020, 106780, ISSN 0098-1354, <https://doi.org/10.1016/j.compchemeng.2020.106780>.
- [23] Shi, J, Chen, G, & Zhu, Y. "Real-Time Natural Gas Leak Detection of Offshore Platforms Using Optical Gas Imaging and Faster R-CNN Approach." *Proceedings of the ASME 2020 39th International Conference on Ocean, Offshore and Arctic Engineering. Volume 1: Offshore Technology*. Virtual, Online. August 3–7, 2020. V001T01A008. ASME. <https://doi.org/10.1115/OMAE2020-19080>
- [24] Ma, P.; Cui, S.; Chen, M.; Zhou, S.; Wang, K. Review of Family-Level Short-Term Load Forecasting and Its Application in Household Energy Management System. *Energies* 2023, 16, 5809. <https://doi.org/10.3390/en16155809>
- [25] Y. LeCun *et al.*, "Backpropagation Applied to Handwritten Zip Code Recognition," in *Neural Computation*, vol. 1, no. 4, pp. 541-551, Dec. 1989, doi: 10.1162/neco.1989.1.4.541.
- [26] Arden Dertat, Applied Deep Learning - Part 4: Convolutional Neural Networks, 2017
- [27] Alex Krizhevsky, Ilya Sutskever, and Geoffrey E. Hinton. 2017. ImageNet classification with deep convolutional neural networks. *Commun. ACM* 60, 6 (June 2017), 84–90. <https://doi.org/10.1145/3065386>
- [28] Alzubaidi L, Zhang J, Humaidi AJ, Al-Dujaili A, Duan Y, Al-Shamma O, Santamaria J, Fadhel MA, Al-Amidie M, Farhan L. Review of deep learning: concepts, CNN architectures, challenges, applications, future directions. *J Big Data*. 2021;8(1):53. doi: 10.1186/s40537-021-00444-8. Epub 2021 Mar 31. PMID: 33816053; PMCID: PMC8010506.
- [29] Jingfan Wang, Lyne P. Tchapmi, Arvind P. Ravikumar, Mike McGuire, Clay S. Bell, Daniel Zimmerle, Silvio Savarese, Adam R. Brandt, Machine vision for natural gas methane emissions detection using an infrared camera, *Applied Energy*, Volume 257, 2020, 113998, ISSN 0306-2619, <https://doi.org/10.1016/j.apenergy.2019.113998>.
- [30] Dennis K. Mikel, Raymond Merrill, Jennifer Colby, Tracey L Footer, Philip Crawford, Laura Alvarez-Aviles (2011), EPA Handbook: Optical Remote Sensing for Measurement and Monitoring of Emissions Flux
- [31] Hagen, N. Survey of autonomous gas leak detection and quantification with snapshot infrared spectral imaging. *J. Opt.* 2020, 22, 103001, DOI 10.1088/2040-8986/abb1cf
- [32] Fox, T.A.; Barchyn, T.E.; Risk, D.; Ravikumar, A.P.; Hugenholtz, C.H. A review of close-range and screening technologies for mitigating fugitive methane emissions in upstream oil and gas. *Environ. Res. Lett.* 2019, 14, 053002, Erratum in *Environ. Res. Lett.* 2019, 14, 069601, DOI 10.1088/1748-9326/ab0cc3

- [33] Teledyne FLIR. Remote Tank Level Monitoring and Gas Detection with AI | Optical Gas Imaging | FLIR. Available online: <https://www.youtube.com/watch?v=oNDg-cNTgMU>
- [34] 1995 Protocol for Equipment Leak Emission Estimates, U.S. ENVIRONMENTAL PROTECTION AGENCY, Office of Air and Radiation, Office of Air Quality Planning and Standards Research Triangle Park, North Carolina 27711, Publication No. EPA-453/R-95-017
- [35] De Almeida, Paulo, Correia, Elliane, and Sonia Quintas. "Detection and Quantification of Gas Leakage by Infrared Technology in TEPA Block 17 FPSOs." Paper presented at the SPE International Conference and Exhibition on Health, Safety, Environment, and Sustainability, Virtual, July 2020. doi: <https://doi.org/10.2118/199519-MS>
- [36] Arvind P Ravikumar *et al*, Repeated leak detection and repair surveys reduce methane emissions over scale of years, 2020 *Environ. Res. Lett.* 15 034029, DOI 10.1088/1748-9326/ab6ae1
- [37] 1995 Protocol for Equipment Leak Emission Estimates, U.S. ENVIRONMENTAL PROTECTION AGENCY Office of Air and Radiation Office of Air Quality Planning and Standards Research Triangle Park, North Carolina 27711, Publication No. EPA-453/R-95-017
- [38] J.I. Connolly, R.A. Robinson, T.D. Gardiner, Assessment of the Bacharach Hi Flow® Sampler characteristics and potential failure modes when measuring methane emissions, *Measurement*, Volume 145, 2019, Pages 226-233, ISSN 0263-2241, <https://doi.org/10.1016/j.measurement.2019.05.055>.
- [39] Al-hilal, H. Saudi Aramco Leak Detection and Repair (LDAR) Program. Available online: <https://www.epa.gov/sites/default/files/2016-04/documents/tue6ldarprogram.pdf>
- [40] F. Gal, W. Kloppmann, E. Proust, P. Humez, Gas concentration and flow rate measurements as part of methane baseline assessment: Case of the Fontaine Ardente gas seep, Isère, France, *Applied Geochemistry*, Volume 95, 2018, Pages 158-171, ISSN 0883-2927, <https://doi.org/10.1016/j.apgeochem.2018.05.019>.
- [41] Jacob G. Englander, Adam R. Brandt, Stephen Conley, David R. Lyon, and Robert B. Jackson; Aerial Interyear Comparison and Quantification of Methane Emissions Persistence in the Bakken Formation of North Dakota, USA. *Environmental Science & Technology* 2018 52 (15), 8947-8953; DOI: 10.1021/acs.est.8b01665
- [42] S. Dierks and A. Kroll, "Quantification of methane gas leakages using remote sensing and sensor data fusion," 2017 IEEE Sensors Applications Symposium (SAS), Glassboro, NJ, USA, 2017, pp. 1-6, doi: 10.1109/SAS.2017.7894047.
- [43] Kohse-Hoinghaus, K., & Jefferies, J.B. (2002). *Applied Combustion Diagnostics* (1st ed.). CRC Press. <https://doi.org/10.1201/9781498719414>
- [44] Miriam Lev-On, Hal Taback, David Epperson, Jeffrey Siegell, Lee Gilmer, Karin Ritter; Methods for quantification of mass emissions from leaking process equipment when using optical imaging for leak detection; *Environmental Progress*, Volume 25, Issue 1, April 2006, Pages 49-55, <https://doi.org/10.1002/ep.10102>
- [45] Srivastava, S., Divekar, A.V., Anilkumar, C. *et al*. Comparative analysis of deep learning image detection algorithms. *J Big Data* 8, 66 (2021). <https://doi.org/10.1186/s40537-021-00434-w>
- [46] Gidaris, Spyros and Nikos Komodakis. "LocNet: Improving Localization Accuracy for Object Detection." *2016 IEEE Conference on Computer Vision and Pattern Recognition (CVPR)* (2015): 789-798.
- [47] Joyce Xu, Deep Learning for Object Detection: A Comprehensive Review, Available online: <https://towardsdatascience.com/deep-learning-for-object-detection-a-comprehensive-review-73930816d8d9>

- [48] Kong Y, Yu T. A Deep Neural Network Model using Random Forest to Extract Feature Representation for Gene Expression Data Classification. *Sci Rep.* 2018 Nov 7;8(1):16477. doi: 10.1038/s41598-018-34833-6. PMID: 30405137; PMCID: PMC6220289.
- [49] Girshick, Ross B. et al. "Rich Feature Hierarchies for Accurate Object Detection and Semantic Segmentation." *2014 IEEE Conference on Computer Vision and Pattern Recognition* (2013): 580-587.
- [50] Aakarsh Yelisetty, Understanding Fast R-CNN and Faster R-CNN for Object Detection, Available online: <https://towardsdatascience.com/understanding-fast-r-cnn-and-faster-r-cnn-for-object-detection-adbb55653d97>
- [51] Rohith Gandhi, R-CNN, Fast R-CNN, Faster R-CNN, YOLO — Object Detection Algorithms, Available online: <https://towardsdatascience.com/r-cnn-fast-r-cnn-faster-r-cnn-yolo-object-detection-algorithms-36d53571365e#:~:text=The%20reason%20%E2%80%9CFast%20R%2DCNN,map%20is%20generated%20from%20it>
- [52] Rohith Gandhi, R-CNN, Fast R-CNN, Faster R-CNN, YOLO — Object Detection Algorithms, Available online: <https://towardsdatascience.com/r-cnn-fast-r-cnn-faster-r-cnn-yolo-object-detection-algorithms-36d53571365e>
- [53] Shilpa Ananth, Faster R-CNN for object detection, Available online: <https://towardsdatascience.com/faster-r-cnn-for-object-detection-a-technical-summary-474c5b857b46>
- [54] Tanay Karmarkar, Region Proposal Network (RPN) — Backbone of Faster R-CNN, Available online: <https://medium.com/@codeplumber/region-proposal-network-rpn-backbone-of-faster-r-cnn-4a744a38d7f9>
- [55] How does thermal imaging work, Available online: <https://www.pyrosales.com.au/blog/news/how-does-thermal-imaging-work/#:~:text=Thermal%20cameras%20detect%20temperature%20by,ways%20that%20heat%20is%20transferred>
- [56] S. Kumar, C. Torres, O. Ulutan, A. Ayasse, D. Roberts and B. S. Manjunath, "Deep Remote Sensing Methods for Methane Detection in Overhead Hyperspectral Imagery," 2020 IEEE Winter Conference on Applications of Computer Vision (WACV), Snowmass, CO, USA, 2020, pp. 1765-1774, doi: 10.1109/WACV45572.2020.9093600.
- [57] Pejčić B, Eadington P, Ross A. Environmental monitoring of hydrocarbons: a chemical sensor perspective. *Environ Sci Technol.* 2007 Sep 15;41(18):6333-42. doi: 10.1021/es0704535. PMID: 17948776.
- [58] Joyce, P., Villena, C.R., Huang, Y., Webb, A., Manuel Gloor, I., Fabien H. Wagner, G., Chipperfield, M.P., Guilló, R.B., Wilson, C., & Hartmut Boesch, H. Using a deep neural network to detect methane point sources and quantify emissions from PRISMA hyperspectral satellite images.
- [59] Methane 'Super-Emitters' Mapped by NASA's New Earth Space Mission, October 25, 2022, Available online: <https://www.nasa.gov/centers-and-facilities/jpl/methane-super-emitters-mapped-by-nasas-new-earth-space-mission/>
- [60] Bobby Pejčić, Peter Eadington, and Andrew Ross, Environmental Monitoring of Hydrocarbons: A Chemical Sensor Perspective, *Environmental Science & Technology* 2007 41 (18), 6333-6342, DOI: 10.1021/es0704535
- [61] Liu, S., Xue, M., Cui, X., & Peng, W. (2023). A review on the methane emission detection during offshore natural gas hydrate production. *Frontiers in Energy Research*, 11, 1130810.

<https://doi.org/10.3389/fenrg.2023.1130810>

[62] Arvind P. Ravikumar, Jingfan Wang, Mike McGuire, Clay S. Bell, Daniel Zimmerle, and Adam R. Brandt, “Good versus Good Enough?” Empirical Tests of Methane Leak Detection Sensitivity of a Commercial Infrared Camera, *Environmental Science & Technology* 2018 52 (4), 2368-2374, DOI: 10.1021/acs.est.7b04945

[63] Stuart N. Riddick, Mercy Mbua, Arthur Santos, Ethan W. Emerson, Fancy Cheptonui, Cade Houlihan, Anna L. Hodshire, Abhinav Anand, Wendy Hartzell, Daniel J. Zimmerle, Methane emissions from abandoned oil and gas wells in Colorado, *Science of The Total Environment*, Volume 922, 2024, 170990, ISSN 0048-9697, <https://doi.org/10.1016/j.scitotenv.2024.170990>.

[64] Townsend-Small, A., Ferrara, T. W., Lyon, D. R., Fries, A. E., & Lamb, B. K. (2016). Emissions of coalbed and natural gas methane from abandoned oil and gas wells in the United States. *Geophysical Research Letters*, 43(5), 2283-2290. <https://doi.org/10.1002/2015GL067623>

[65] Sherwin ED, Rutherford JS, Chen Y, Aminfarid S, Kort EA, Jackson RB, Brandt AR. Single-blind validation of space-based point-source detection and quantification of onshore methane emissions. *Sci Rep.* 2023 Mar 7;13(1):3836. doi: 10.1038/s41598-023-30761-2. PMID: 36882586; PMCID: PMC9992358.

[66] Allen DT, Torres VM, Thomas J, Sullivan DW, Harrison M, Hendler A, Herndon SC, Kolb CE, Fraser MP, Hill AD, Lamb BK, Miskimins J, Sawyer RF, Seinfeld JH. Measurements of methane emissions at natural gas production sites in the United States. *Proc Natl Acad Sci U S A.* 2013 Oct 29;110(44):17768-73. doi: 10.1073/pnas.1304880110. Epub 2013 Sep 16. Erratum in: *Proc Natl Acad Sci USA.* 2013 Oct 29;110(44):18023. PMID: 24043804; PMCID: PMC3816463.

[67] Jenna A. Brown, Matthew R. Harrison, Tecle Rufael, Selina A. Roman-White, Gregory B. Ross, Fiji C. George, and Daniel Zimmerle, Informing Methane Emissions Inventories Using Facility Aerial Measurements at Midstream Natural Gas Facilities, *Environmental Science & Technology* 2023 57 (39), 14539-14547, DOI: 10.1021/acs.est.3c01321

[68] Thoma ED, Deshmukh P, Logan R, Stovern M, Dresser C, Brantley HL. Assessment of Uinta Basin Oil and Natural Gas Well Pad Pneumatic Controller Emissions. *J Environ Prot (Irvine, Calif).* 2017 Apr;8(4):394-415. doi: 10.4236/jep.2017.84029. PMID: 30319880; PMCID: PMC6178829.

[69] Zimmerle D, Vaughn T, Luck B, Lauderdale T, Keen K, Harrison M, Marchese A, Williams L, Allen D. Methane Emissions from Gathering Compressor Stations in the U.S. *Environ Sci Technol.* 2020 Jun 16;54(12):7552-7561. doi: 10.1021/acs.est.0c00516. Epub 2020 Jun 1. PMID: 32407076.

[70] Anthony J. Marchese, Timothy L. Vaughn, Daniel J. Zimmerle, David M. Martinez, Laurie L. Williams, Allen L. Robinson, Austin L. Mitchell, R. Subramanian, Daniel S. Tkacik, Joseph R. Roscioli, and Scott C. Herndon, Methane Emissions from United States Natural Gas Gathering and Processing, *Environmental Science & Technology* 2015 49 (17), 10718-10727, DOI: 10.1021/acs.est.5b02275

[71] Strahl T, Herbst J, Lambrecht A, Maier E, Steinebrunner J, Wöllenstein J. Methane leak detection by tunable laser spectroscopy and mid-infrared imaging. *Appl Opt.* 2021 May 20;60(15):C68-C75. doi: 10.1364/AO.419942. PMID: 34143108.

[72] Renee McVay, METHANE EMISSIONS FROM U.S. GAS PIPELINE LEAKS, August 2023, Environmental Defense Fund.

[73] Yudaya Sivathanu, Technology Status Report on Natural Gas Leak Detection in Pipelines, Prepared for U.S. Department of Energy.

- [74] Weil, Gary J. "Non Contact, Remote Sensing of Buried Water Pipeline Leaks Using Infrared Thermography." (1993).
- [75] Kulp, Thomas J. , Powers, Peter E. , Kennedy, Randall B., Remote imaging of controlled gas releases using active and passive infrared imaging systems, August 1997, DOI: 10.1117/12.280321
- [76] Mark L.G. Althouse, Chein-I Chang, Chemical vapor detection with a multispectral thermal imager, Optical Engineering 30(11), 1725-1733 (November 1991)
- [77] Kang, R.; Liatsis, P.; Kyritsis, D.C. Emission Quantification via Passive Infrared Optical Gas Imaging: A Review. *Energies* 2022, 15, 3304. <https://doi.org/10.3390/en15093304>
- [78] Charles L. Bennett, Michael R. Carter, and David J. Fields "Hyperspectral imaging in the infrared using LIFTIRS", Proc. SPIE 2552, Infrared Technology XXI, (8 September 1995); <https://doi.org/10.1117/12.218227>
- [79] Zhou, J., Al Hussein, D., Li, J. *et al.* Detection of volatile organic compounds using mid-infrared silicon nitride waveguide sensors. *Sci Rep* 12, 5572 (2022). <https://doi.org/10.1038/s41598-022-09597-9>
- [80] Smith, B. W., "IRISHS: the infrared imaging spatial heterodyne spectrometer: a new pushbroom Fourier transform ultraspectral imager with no moving parts", in *Infrared Technology and Applications XXV*, 1999, vol. 3698, pp. 501–509. doi:10.1117/12.354552.
- [81] Lorenzo-Bayona, J.L.; León, D.; Amez, I.; Castells, B.; Medic, L. Experimental Comparison of Functionality between the Main Types of Methane Measurement Sensors in Mines. *Energies* 2023, 16, 2207. <https://doi.org/10.3390/en16052207>
- [82] Gageik, Nils, Paul Benz and Sergio Montenegro. "Obstacle Detection and Collision Avoidance for a UAV With Complementary Low-Cost Sensors." *IEEE Access* 3 (2015): 599-609.
- [83] Papale, L.G.; Guerrisi, G.; De Santis, D.; Schiavon, G.; Del Frate, F. Satellite Data Potentialities in Solid Waste Landfill Monitoring: Review and Case Studies. *Sensors* 2023, 23, 3917. <https://doi.org/10.3390/s23083917>
- [84] Ling JYX, Chan YJ, Chen JW, Chong DJS, Tan ALL, Arumugasamy SK, Lau PL. Machine learning methods for the modelling and optimisation of biogas production from anaerobic digestion: a review. *Environ Sci Pollut Res Int.* 2024 Mar;31(13):19085-19104. doi: 10.1007/s11356-024-32435-6. Epub 2024 Feb 20. PMID: 38376778.
- [85] Manjunatha GS, Lakshmikanthan P, Chavan D, Baghel DS, Kumar S, Kumar R. Detection and extinguishment approaches for municipal solid waste landfill fires: A mini review. *Waste Manag Res.* 2024 Jan;42(1):16-26. doi: 10.1177/0734242X231168797. Epub 2023 May 6. PMID: 37148210.
- [86] Brovkina, O., Kopkáně, D., Polák, M., Bednařík, A., and Hanuš, J.: APPLICATION OF AIRBORNE DATA TO MONITOR URBAN INFRASTRUCTURE OBJECTS, *Int. Arch. Photogramm. Remote Sens. Spatial Inf. Sci.*, XLVIII-5/W2-2023, 25–29, <https://doi.org/10.5194/isprs-archives-XLVIII-5-W2-2023-25-2023>, 2023.
- [87] Xiao, C.; Fu, B.; Shui, H.; Guo, Z.; Zhu, J. Detecting the Sources of Methane Emission from Oil Shale Mining and Processing Using Airborne Hyperspectral Data. *Remote Sens.* 2020, 12, 537. <https://doi.org/10.3390/rs12030537>
- [88] Andrew K. Thorpe, Christopher O'Handley, George D. Emmitt, Philip L. DeCola, Francesca M. Hopkins, Vineet Yadav, Abhinav Guha, Sally Newman, Jorn D. Herner, Matthias Falk, Riley M. Duren, Improved methane emission estimates using AVIRIS-NG and an Airborne Doppler Wind Lidar, *Remote Sensing of Environment*, Volume 266, 2021, 112681, ISSN 0034-4257, <https://doi.org/10.1016/j.rse.2021.112681>.

- [89] Mayorova V, Morozov A, Golyak I, Golyak I, Lazarev N, Melnikova V, Rachkin D, Svirin V, Tenenbaum S, Vintaykin I, Anfimov D, Fufurin I. Determination of Greenhouse Gas Concentrations from the 16U CubeSat Spacecraft Using Fourier Transform Infrared Spectroscopy. *Sensors (Basel)*. 2023 Jul 29;23(15):6794. doi: 10.3390/s23156794. PMID: 37571577; PMCID: PMC10422423.
- [90] Kim, J., Kim, J., and Jang, S. H., "Infrared spectra in air pollution research and monitoring from space: a review", in *Nano-, Bio-, Info-Tech Sensors and Wearable Systems*, 2021, vol. 11590, Art. no. 115900P. doi:10.1117/12.2584500.
- [91] Lewis AW, Yuen ST, Smith AJ. Detection of gas leakage from landfills using infrared thermography--applicability and limitations. *Waste Manag Res*. 2003 Oct;21(5):436-47. doi: 10.1177/0734242X0302100506. PMID: 14661891.
- [92] Fjelsted L, Christensen AG, Larsen JE, Kjeldsen P, Scheutz C. Assessment of a landfill methane emission screening method using an unmanned aerial vehicle mounted thermal infrared camera - A field study. *Waste Manag*. 2019 Mar 15;87:893-904. doi: 10.1016/j.wasman.2018.05.031. Epub 2018 May 28. PMID: 29853253.
- [93] G Tanda *et al* 2017 *J. Phys.: Conf. Ser.* 796 012016 DOI 10.1088/1742-6596/796/1/012016
- [94] Rodrigues MC, Silveira EA, Brasil Junior ACP. On the correlation between thermal imagery and fugitive CH₄ emissions from MSW landfills. *Waste Manag*. 2023 Jul 1; 166:163-170. doi: 10.1016/j.wasman.2023.05.005. Epub 2023 May 10. PMID: 37172517.
- [95] Xinmei Tian, Siyuan Huang, Luochun Wang, Lin Li, Ziyang Lou, Shouqiang Huang, Zhen Zhou, Mitigation of low methane content landfill gas through visible-near-infrared photocatalysis over Y₂O₃:Er³⁺/Graphene/TiO₂, *Applied Surface Science*, Volume 456, 2018, Pages 854-860, ISSN 0169-4332, <https://doi.org/10.1016/j.apsusc.2018.06.138>.
- [96] Njoku, P.O.; Piketh, S.; Makungo, R.; Edokpayi, J.N. Monitoring of Subsurface Emissions and the Influence of Meteorological Factors on Landfill Gas Emissions: A Case Study of a South African Landfill. *Sustainability* 2023, 15, 5989. <https://doi.org/10.3390/su15075989>
- [97] Gabriela Iorga, 2016. "Air Pollution Monitoring: A Case Study from Romania," Chapters, in: Philip John Sallis (ed.), *Air Quality - Measurement and Modeling*, IntechOpen., DOI: 10.5772/64919
- [98] Peter Werle, Franz Slemr, Karl Maurer, Robert Kormann, Robert Mücke, Bernd Jänker, Near- and mid-infrared laser-optical sensors for gas analysis, *Optics and Lasers in Engineering*, Volume 37, Issues 2–3, 2002, Pages 101-114, ISSN 0143-8166, [https://doi.org/10.1016/S0143-8166\(01\)00092-6](https://doi.org/10.1016/S0143-8166(01)00092-6).
- [99] Ulrike Willer, Mohammad Saraji, Alireza Khorsandi, Peter Geiser, Wolfgang Schade, Near- and mid-infrared laser monitoring of industrial processes, environment and security applications, *Optics and Lasers in Engineering*, Volume 44, Issue 7, 2006, Pages 699-710, ISSN 0143-8166, <https://doi.org/10.1016/j.optlaseng.2005.04.015>.
- [100] Tittel, F.K., Richter, D., Fried, A. (2003). Mid-Infrared Laser Applications in Spectroscopy. In: Sorokina, I.T., Vodopyanov, K.L. (eds) *Solid-State Mid-Infrared Laser Sources*. Topics in Applied Physics, vol 89. Springer, Berlin, Heidelberg. https://doi.org/10.1007/3-540-36491-9_1
- [101] Bley, W. G. Methods of Leak Detection. 907-942. <https://doi.org/10.1002/9783527688265.ch19>
- [102] Li, J.; Yu, Z.; Du, Z.; Ji, Y.; Liu, C. Standoff Chemical Detection Using Laser Absorption Spectroscopy: A Review. *Remote Sens*. 2020, 12, 2771. <https://doi.org/10.3390/rs12172771>
- [103] Mikolajczyk, Janusz; Wojtas, Jacek; Bielecki, Zbigniew; Stacewicz, Tadeusz; Szabra, Dariusz; Magryta,

Pawel; Prokopiuk, Artur; Tkacz, Arkadiusz; Panek, Malgorzata. *Metrology and Measurement Systems; Warsaw* Vol. 23, Iss. 3, (2016): 481-489. DOI:10.1515/mms-2016-0030

[104] Wojtas J, Mikolajczyk J, Bielecki Z. Aspects of the application of cavity enhanced spectroscopy to nitrogen oxides detection. *Sensors (Basel)*. 2013 Jun 10;13(6):7570-98. doi: 10.3390/s130607570. PMID: 23752566; PMCID: PMC3715239.

[105] Allen MG. Diode laser absorption sensors for gas-dynamic and combustion flows. *Meas Sci Technol*. 1998 Apr;9(4):545-62. doi: 10.1088/0957-0233/9/4/001. PMID: 11543363.

[106] Peter Werle, Franz Slemr, Karl Maurer, Robert Kormann, Robert Mücke, Bernd Jänker, Near- and mid-infrared laser-optical sensors for gas analysis, *Optics and Lasers in Engineering*, Volume 37, Issues 2–3, 2002, Pages 101-114, ISSN 0143-8166, [https://doi.org/10.1016/S0143-8166\(01\)00092-6](https://doi.org/10.1016/S0143-8166(01)00092-6).

[107] Sigrist, M., Bartlome, R., Marinov, D. *et al.* Trace gas monitoring with infrared laser-based detection schemes. *Appl. Phys. B* 90, 289–300 (2008). <https://doi.org/10.1007/s00340-007-2875-4>

[108] J. Barry McManus, Mark S. Zahniser, David D. Nelson Jr., Joanne H. Shorter, Scott C. Herndon, Ezra C. Wood, Rick Wehr, "Application of quantum cascade lasers to high-precision atmospheric trace gas measurements," *Opt. Eng.* 49(11) 111124 (1 November 2010) <https://doi.org/10.1117/1.3498782>

[109] Kun Liu, Lei Wang, Tu Tan, Guishi Wang, Weijun Zhang, Weidong Chen, Xiaoming Gao,

Highly sensitive detection of methane by near-infrared laser absorption spectroscopy using a compact dense-pattern multipass cell, *Sensors and Actuators B: Chemical*, Volume 220, 2015, Pages 1000-1005, ISSN 0925-4005, <https://doi.org/10.1016/j.snb.2015.05.136>.

[110] Marc-Simon Bahr, Bernd Baumann, Marcus Wolff, Determining the most suitable spectral range for TDLS – a quantitative approach, *Journal of Quantitative Spectroscopy and Radiative Transfer*, Volume 286, 2022, 108216, ISSN 0022-4073, <https://doi.org/10.1016/j.jqsrt.2022.108216>.

[111] Kwaśny, M.; Bombalska, A. Optical Methods of Methane Detection. *Sensors* 2023, 23, 2834. <https://doi.org/10.3390/s23052834>

[112] Compared with electrochemical or Catalytic type sensors, what are the advantages of laser type sensors?, Available online: <https://www.dlactech.com/faq-en.html>

[113] Thermal camera or laser methane detector (U10)?, Available online: <https://www.drone-thermal-camera.com/thermal-camera-or-laser-methane-detector-u10/>

[114] Methane Gas Detection: Thermal vs Laser, Available online: <https://nextech.online/methane-gas-detection/#:~:text=Infrared%20sensors%20detect%20a%20wider,automatically%20detect%20the%20relevant%20gas>